A simulation of soil water content based on remote sensing in a semi-arid Mediterranean agricultural landscape

N. Sánchez[1],*, J. Martínez-Fernández[1], M. Rodríguez-Ruiz[1], E. Torres[2] and A. Calera[2]

[1] Centro Hispano-Luso de Investigaciones Agrarias (CIALE). Universidad de Salamanca.
Río Duero, 12, 37185 Villamayor (Salamanca), Spain
[2] Instituto de Desarrollo Regional (IDR). Universidad de Castilla-La Mancha, Campus Universitario s/n,
02071 Albacete, Spain

Abstract

This paper shows the application of a water balance based on remote sensing that integrated a Landsat 5 series from 2009 in an area of 1,300 km² in the Duero Basin (Spain). The objective was to simulate the daily soil water content (SWC), actual evapotranspiration, deep percolation and irrigation rates. The accuracy of the application is tested in a semi-arid Mediterranean agricultural landscape with crops over natural conditions. The results of the simulated SWC were compared against 19 *in situ* stations of the Soil Moisture Measurement Stations Network (REMEDHUS), in order to check the feasibility and accuracy of the application. The theoretical basis of the application was the FAO56 calculation assisted by remotely sensed imagery. The basal crop coefficient (K_{cb}), as well as other parameters of the calculation came from the remote reflectance of the images. This approach was implemented in the computerized tool HIDROMORE+, which integrates various spatial databases. The comparison of simulated and observed values (at different depths and different land uses) showed a good global agreement for the area ($R^2 = 0.92$, RMSE = 0.031 m³ m⁻³, and bias = –0.027 m³ m⁻³). The land uses better described were rainfed cereals ($R^2 = 0.86$, RMSE = 0.030 m³ m⁻³, and bias = –0.025 m³ m⁻³) and vineyards ($R^2 = 0.86$, RMSE = 0.016 m³ m⁻³, and bias = –0.013 m³ m⁻³). In general, an underestimation of the soil water content is noticed, more pronounced into the root zone than at surface layer. The final aim was to convert the application into a hydrological tool available for agricultural water management.

Additional key words: crop coefficient; evapotranspiration; Landsat 5; NDVI; water balance.

Resumen

Simulación del contenido de agua del suelo mediante teledetección en un contexto semiárido mediterráneo

Este trabajo muestra la aplicación de un balance de agua basado en teledetección que integra una serie Landsat 5 de 2009, en una zona de 1.300 km² de la cuenca del Duero (España). El objetivo fue la simulación diaria de contenido de agua del suelo, evapotranspiración real, percolación profunda y tasas de riego. La precisión fue comprobada en el contexto agrícola mediterráneo, en cultivos bajo condiciones naturales. Los resultados acerca del contenido de agua en el suelo se compararon con 19 estaciones de la Red de Estaciones de Medición de Humedad de Suelo (REMEDHUS). La base teórica de la aplicación es FAO56 combinado con imágenes de satélite. El coeficiente de cultivo basal y otros parámetros del cálculo se obtuvieron mediante la reflectividad de las imágenes. Todo ello se implementó en una herramienta informática, HIDROMORE+, capaz de gestionar las bases de datos espaciales. La comparación del contenido de humedad simulado con el observado a diferentes profundidades y distintos usos de suelo, muestra un buen ajuste global ($R^2 = 0,92$; RMSE = 0,031 m³ m⁻³; y bias = –0,027 m³ m⁻³). Por usos de suelo, el mejor descrito fue el de cereales en régimen de secano ($R^2 = 0,86$; RMSE = 0,030 m³ m⁻³; y bias = –0,025 m³ m⁻³) y la viña ($R^2 = 0,86$; RMSE = 0,016 m³ m⁻³; y bias = –0,013 m³ m⁻³). En general, el contenido de agua en el suelo fue subestimado, lo que es más evidente en la zona de raíces que en la capa superficial. El objetivo final es convertir la aplicación en una herramienta hidrológica para la gestión del agua en agricultura.

Palabras clave adicionales: balance de agua; coeficiente de cultivo; evapotranspiración; Landsat 5; NDVI.

Abbreviations used: AET (actual evapotranspiration); ET₀ (reference evapotranspiration); GIS (geographic information system); Kc (crop coefficient); Kcb (basal crop coefficient); NDVI (normalized difference vegetation index); REMEDHUS (Soil Moisture Measurement Stations Network); SIGPAC (geographic information system for agricultural plots); SMAP (soil moisture active passive); SMOS (soil moisture and ocean salinity); SWC (soil water content).

Introduction

Soil water content (SWC) is a highly dynamic ecological variable, but it is also one of the most sensitive factors in agricultural yield. In semi-arid Mediterranean areas, where water scarcity is a common situation, SWC is the limiting factor for agriculture, and crop evapotranspiration is the main factor of water consumption. Accurate information on SWC is crucial for practical agricultural water management at various scales (Ju *et al.*, 2010). Point measurements of SWC are frequent in agricultural areas for controlling irrigation scheduling and water reserves (Bonet *et al.*, 2010), either with measurements at different depths or with a water balance using the crop coefficient-reference evapotranspiration (K_c-ET_0) approach (Allen *et al.*, 1998). However, the spatial heterogeneity of soil properties makes it difficult to scale up measurements from points to large scales, and spatial monitoring designs are costly and time-consuming (Western & Grayson, 2000). This is a difficult problem for agricultural water management, and several remote sensing spatial missions (such as AMSR-E, ERS, SMOS, and SMAP) have attempted to fill this gap, even though improved process understanding and algorithms are needed to enable the use of these data in the future (Wagner *et al.*, 2007a).

The application of hydrological models to simulate SWC with adequate accuracy in heterogeneous and complex areas remains challenging, and the utmost efforts should be made to exactly determine fine-scale meteorological data and to build a spatial skeleton to improve soil moisture modeling (Rößler & Löffler, 2010). The possibility of producing maps of hydrological variables by combining a mass balance approach and remotely sensed data to calculate a water budget is a useful tool for watershed-level hydrologic models (Earls *et al.*, 2006) because the water balance provides high temporal resolution, whereas the remote sensing approach provides high spatial coverage. It is thus possible to monitor crop status and water use through remotely sensed crop coefficients in a dynamic manner for every plot. The crop coefficients derived from the vegetation index (Bausch & Neale, 1987; Neale *et al.*, 1989; Calera *et al.*, 2004; Gonzalez-Dugo & Mateos, 2008; Er-Raki *et al.*, 2010) account for any situation out of pristine growing conditions of climate, management or vegetative vigor.

The FAO56 water balance (Allen *et al.*, 1998) has been used in recent works both at point scale (Allen, 2000; Hunsaker *et al.*, 2005; Er-Raki *et al.*, 2007; López-Urrea *et al.*, 2009; Campos *et al.*, 2010; Liu & Luo, 2010; Torres & Calera, 2010) and spatially distributed (Zhang & Wegehenkel, 2006; Er-Raki *et al.*, 2010; Sánchez *et al.*, 2010). The use of a linear relationship of NDVI-K_{cb} (Normalized Difference Vegetation Index-basal crop coefficient) instead of the tabulated values of K_{cb} improves the accuracy of the results, even over woody crops, as shown in Campos *et al.* (2010). Another promising aspect for using the NDVI-based K_{cb} is its ability to provide a direct approach to determining actual evapotranspiration (AET) conditions when crop growth and water use deviate from optimum conditions (Hunsaker *et al.*, 2005).

The second basic approach in the application is using a map of land use/land cover extracted from an image classification method. The map can produce spatial distributions of some calculation parameters assigned to each of its classes.

In areas where irrigation rates must be controlled precisely, where it is essential to prevent water loss, one approach to check if the supply is adequate to meet the demand is to account for the respective components in the water balance (Singh *et al.*, 2010). In this sense, irrigation advisory systems show increasing success in different regions of Spain and the world based on climate information, crop status, and agricultural practices (Martín de Santa Olalla *et al.*, 2003).

This work aims to demonstrate the reliability of the combination of remote sensing with a hydrologic balance model to obtain hydrological variables in a distributed manner. For this proposal, this work compares the results of SWC simulated against *in situ* measured values. A second objective is to demonstrate the accuracy of this straightforward method so that it can be implemented as a query tool for farmers and managers of water, who in the future could use it to obtain near real-time data of crops and water requirements. Here, the water balance is implemented in a spatially distributed tool, HIDRO-MORE+, which was previously tested in the same area in 2001 and 2002 (Sánchez *et al.*, 2010).

Material and methods

Brief description of the study area and the climatic conditions

The Soil Moisture Measurement Stations Network (REMEDHUS) is made up of 19 stations for the measurement and monitoring of soil moisture and three
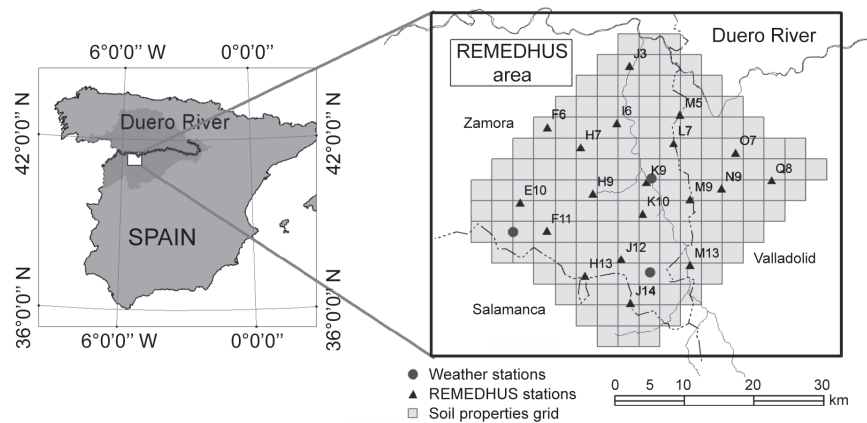
Figure 1. Study area location and REMEDHUS network (soils grid, soil moisture network, and weather stations).

automatic weather stations among other equipment for hydrological and climatic monitoring (Martínez-Fernández & Ceballos, 2003, 2005). These stations are located in an area of approximately 1,300 km² (41.1° –41.5° N; –5.1° –5.7° W) in a central semi-arid part of the Duero Basin (Fig. 1). This area is nearly flat, ranging from 700 to 900 m a.s.l. The climate is continental semiarid Mediterranean. The land uses are mainly agricultural: rainfed cereals in winter and spring (78%), irrigated crops in summer (5%), and vineyards (3%). There are also some patchy areas of mixed forests and pastures (13%). The most abundant soils are Luvisols and Cambisols with a predominantly sandy texture (mean sand content, 71%) (Martínez-Fernández & Ceballos, 2003).

In the year of study (2009), the rainfall was 332.1 mm, and the ET_0 (FAO56-Penmann-Monteith method) was 1,147.6 mm. The monthly data (Fig. 2) show a water deficit for all months except December and January. ET_0 is especially high in the summer period.

Input data and pre-treatment

The simulation was performed along 2009 at daily interval. Three datasets were needed for the calculation: meteorological information (*i.e.,* daily precipitation and ET_0), imagery (*i.e.,* NDVI time series and a map of land use-land cover), and spatially distributed soil information.

Daily precipitation and ET_0, were computed from the automatic weather stations (Fig. 1). HIDRO-MORE+ performs a spatial interpolation based on the Inverse Distance Weighting method (Shepard, 1968).

The imagery came from Landsat 5 TM (scene 202-031). In 2009, three images were selected after discarding cloudy images: March 23, June 11, and August 30. These dates covered the most significant periods of the crop growing cycles under study, *i.e.,* spring for rainfed cereals and summer for irrigated crops and vineyards. The images were orthorectified and registered by a rigorous model (Toutin, 2004) with 20 ground control points, plus the elevation digital model and the orbital information. This process guarantees the spatial coincidence of the three scenes. Radiometric calibration and atmospheric correction were also performed by means of the standard values of the atmosphere and the dark object subtraction method (Chavez, 1989). The NDVI (Rouse *et al.*, 1974) was calculated as the normalized difference between infrared and red physical units, *i.e.,* the
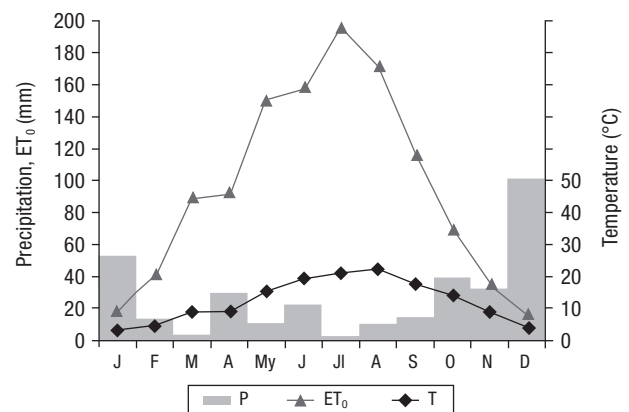
Figure 2. Climatic characteristics of 2009 averaged from the three weather stations in the study area. P, precipitation; ET_0, reference evapotranspiration; T, temperature.

reflectance at-surface resulting from the radiometric and atmospheric treatment. The composite image of the three NDVI become the input for the classification process and the basis for computing K_{cb} as well as the fraction of vegetation cover and other parameters of the calculation.

For the classification, a hybrid method was used that mixed the Geographic Information System (GIS) for Agricultural Plots of Castilla y León Region (SIGPAC) with the NDVI composite. This process comprised two steps. First, the SIGPAC plots of water, urban, forest-pasture and vineyards were clipped from the image. Second, to separate the mixed category 'arable land', a segmentation procedure of the NDVI levels was performed (Vincent & Pierre, 2003), which allowed the segmentation of rainfed, irrigated and fallow areas, taking advantage of the opposite growing cycle of all of them. The union of the results of both steps became the land use/land cover map (Fig. 3). The accuracy assessment with ground truth areas showed a coincidence of 100% for water, 85.7% for forest-pasture, 76.5% for vineyard, 84.6% for rainfed cereals, 100% for irrigated crops and 90% for fallow. The average

accuracy was 86.8%. This map established some parameters of the water balance for each class (or restrict some others), such as root depth, plant height, and thresholds of K_{cb}.

Finally, for the soil database required for the calculation, soil samples at surface level (0-5 cm) were collected in a grid basis (cells of 3 km × 3 km). The SWC at field capacity (SWC_{FC}) and at wilting point (SWC_{WP}) were determined for the center of 146 cells. The water retention curve was obtained in laboratory measurements on these undisturbed soil samples (100 cm^3 monoliths) taken at the surface layer in the center of each cell. The method combines tension boxes (sand box method) for potentials close to zero and membrane pressure method for low tension conditions. Using this combined method nine experimental points (soil moisture *vs.* tension pairs) of the soil retention curve were obtained at 0, 0.2, 1, 3, 10, 30, 100, 300, and 1,500 kP. After the adjusting to an empirical model (van Genuchten, 1980) one can obtain the entire curve and then obtain parameters as field capacity (−33 kPa for SWC_{FC}), wilting point (−1,500 kPa for SWC_{WP}), saturation or so on.
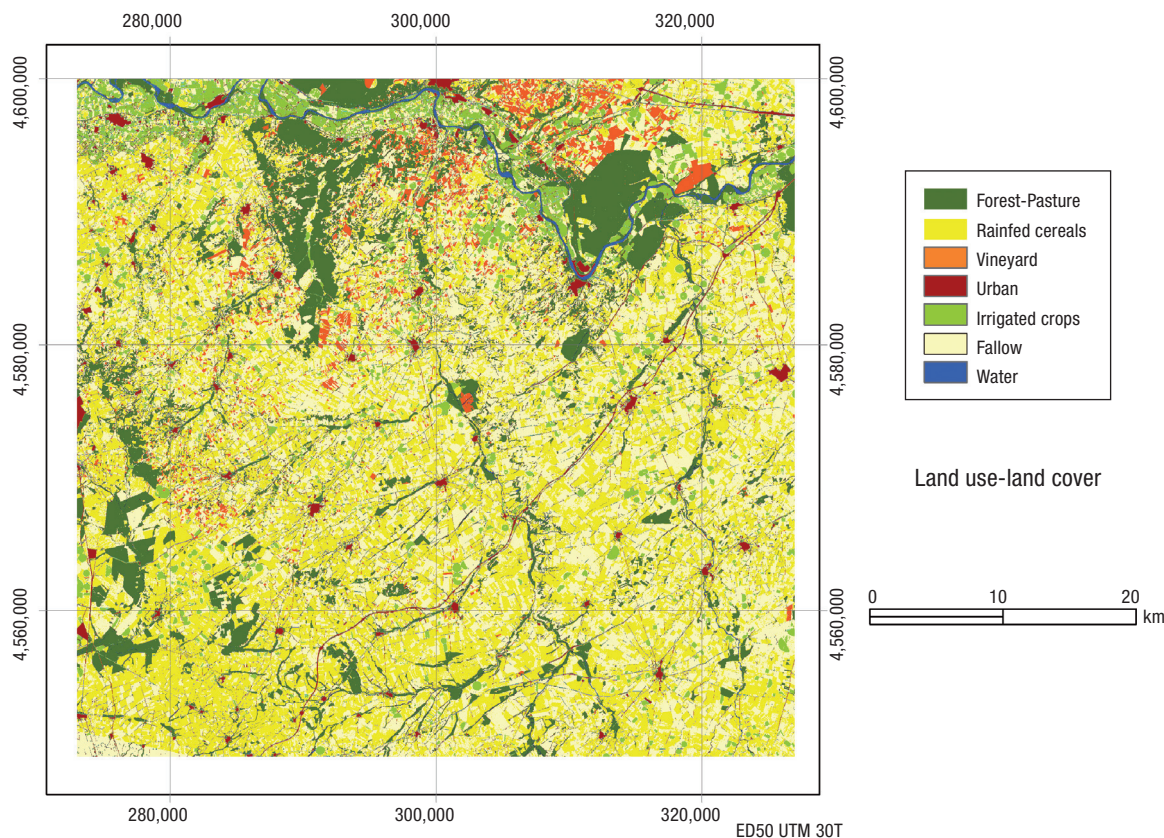

Figure 3. Land use/land cover map.

Calculation basis

The K_c-ET_0 approach uses meteorological data and crop coefficients to calculate crop evapotranspiration. The dual form of K_c was chosen (Wright, 1982), as is developed in FAO56:

$$AET = ET_0 (K_s K_{cb} + K_e) \qquad [1]$$

The term $ET_0 K_s K_{cb}$ represents the transpiration component from the plants, and the term $ET_0 K_e$, represents the evaporation component from the soil. K_{cb} is the transpiration coefficient at a potential rate, *i.e.,* when water is not limiting transpiration, and it is usually obtained from tabulated values; here, it was calculated as a linear form of the NDVI (Bausch & Neale, 1987):

$$K_{cb} = 1.36 \, NDVI-0.03 \qquad [2]$$

K_s describes the effect of water stress, and it is calculated according the water content in the root layer, estimated from the daily water balance. The soil evaporation coefficient, K_e, is calculated from the daily water balance on the upper soil surface layer (10 cm). Thus, the calculation accounts for the effective root zone, but the upper topsoil is considered during the non-growing periods or over bare soil conditions (*i.e.,* fallow). This daily balance, the coefficients calculation, and the limits of available soil water content are described by Allen *et al.* (1998) and Allen (2000).

SWC can be calculated as the residual of the daily water balance. It is expressed in volumetric units and is analyzed in terms of plant available water. FAO56 establishes the SWC_{FC} as the upper limit, and the remaining SWC is calculated as the difference between the water at field capacity and the water deficit or depletion (the residual of the balance). HIDROMORE+ establishes the SWC_{WP} as the minimum SWC.

Comparison methods and alternatives

Hydrological models are mainly calibrated and validated using runoff (Rößler & Löffler, 2010) or evapotranspiration (Allen, 2000; Eitzinger *et al.*, 2002; Er-Raki *et al.*, 2007). However, because runoff processes do not provide much insight into internal processes (Grayson *et al.*, 1992a,b) soil moisture simulations also need to be validated. Regarding this validation purpose, the REMEDHUS network performs a continuous measurement of 0-5 cm soil moisture in 19 stations with one Hydra Probe (Stevens® Water Monitoring System, Inc.), and at different depths with an EnviroSMART™ soil water profile (Sentek Technologies) installed in 12 stations. The EnviroSMART probes can include several sensors that measure soil water at multiple depths, customized for individual applications by adding sensors at user-specified measurement. In REMEDHUS, three probes at 25, 50 and 100 cm depths were installed. Hydra and EnviroSMART are capacitance probes which measure soil dielectric constant to calculate soil moisture content. At each station sensors are connected to a CR200 (Campbell Scientific Ltd.) datalogger where soil moisture data are stored at hourly intervals. As stated before, there were 19 Hydra stations in that period; among them, 12 also had EnviroSMART profiles.

The hydraulic properties were obtained in the laboratory in a similar procedure as the soil grid, *i.e.,* after taking undistorted soil samples at the different depths in each station. SWC_{FC}, SWC_{WP} and SWC at saturation (SWC_{sat}) were determined. For the validation process, taking into account that water balance considers the SWC at root depth, profile-average values were considered as well as the root depth for each land use/land cover (Table 1).

The alternatives considered for the SWC validation were the following: a) using the surface SWC observed in the Hydraprobe stations (SWC_{hyd}); b) using the profile-averaged SWC resulting from the EnviroSMART profiles (SWC_{env}); c) using the profile-averaged SWC of all sensors (one at surface and three along the profile), SWC_{all}.

Six stations under rainfed cereals, five under vineyards, five under fallow and three under forest-pasture were used. The validation strategy consisted in comparing simulated and observed values using the coefficient of determination (R^2), bias, and the root mean square error (RMSE), namely:

$$bias = SWC_{SIMi} - SWC_{OBSi}$$

$$RMSE = \sqrt{\frac{1}{N} \sum_{i=1}^{N} (SWC_{SIMi} - SWC_{OBSi})^2}$$

where the bias represents the deviation or difference between the simulated SWC and the observed series of SWC (SWC_{hyd}, SWC_{env}, and SWC_{all}) for each day *i*; and the RMSE represents the cuadratic mean of these differences along the time series. These statistics were applied for each station, as well as for the land use-averaged SWC and total-averaged SWC of the whole area.

Table 1. Profile-averaged hydraulic soil parameters (SWC_{FC}, soil water content at field capacity, SWC_{WP}, soil water content at wilting point, and SWC_{SAT}, soil water content at at saturation) at the REMEDHUS stations. Land uses and type of soil moisture sensor are also indicated

Station	Type[1]	Land use[2]	SWC_{FC} (m³ m⁻³)	SWC_{WP} (m³ m⁻³)	SWC_{SAT} (m³ m⁻³)	Z_r (m)
E10	H + E	V	0.157	0.074	0.386	1.00
F11	H	R	0.093	0.035	0.387	0.10 to 0.90
F6	H + E	V	0.167	0.096	0.329	1.00
H7	H + E	V	0.085	0.043	0.386	1.00
H13	H + E	F	0.124	0.070	0.438	0.10
H9	H + E	F–P	0.235	0.153	0.461	2.00
I6	H + E	V	0.085	0.052	0.347	1.00
J12	H + E	F	0.227	0.121	0.443	0.10
J3	H	V	0.053	0.022	0.367	1.00
J14	H + E	F	0.163	0.075	0.420	0.10
K10	H	R	0.070	0.027	0.369	0.10 to 0.90
K9	H	F–P	0.189	0.095	0.446	2.00
L7	H	R	0.290	0.176	0.511	0.10 to 0.90
M5	H + E	R	0.095	0.051	0.408	0.10 to 0.90
M13	H	F–P	0.344	0.195	0.438	2.00
M9	H + E	R	0.238	0.146	0.512	0.10 to 0.90
N9	H + E	F	0.268	0.146	0.530	0.10
O7	H + E	R	0.118	0.060	0.459	0.10 to 0.90
Q8	H	F	0.194	0.125	0.467	0.10

[1] H, Hydra; E, EnviroSMART. [2] V, vineyard; R, rainfed cereals; F, fallow; FP, forest-pasture, root depth (Z_r).

Results

The simulated SWC was compared against the observed following the three alternatives of validation (Fig. 4, only one station representative of each category is shown). The vineyard soils took small SWC values along the year (Fig. 4a). These soils have more content of sand and thus less retention capacity, and there are no differences among the observed values along the profile. The simulated SWC curves and the observed curves matched perfectly. Therefore, for the other categories, there are greater differences between SWC_{hyd}, SWC_{env}, and SWC_{all}. Among these differences, as expected, the behavior of SWC_{hyd} fluctuates more because it is a surface layer content; this fact is more evident in the rainfed cereal (Fig. 4b). The failure of the simulation of fallow lands is noticeable (Fig. 4c). Because the calculation does not consider plant activity, but only the evaporation layer, the depletion is the maximum and SWC equals the minimum value, SWC_{WP}.

For the simulated SWC, a slight underestimation compared with the observed values can be seen in all categories, especially if comparing SWC_{hyd} with the forest-pasture cover (Fig. 4d). The observed SWC is greater in forest-pastures due to their location in the valley bottoms, where the water table is shallow in winter, floods sometimes occur, and there is a higher content of clay in the soils. It should be pointed out that the calculation establishes the upper limit of the simulated SWC as SWC_{FC}, but the curve indicates that the actual SWC on the soils exceeds this limit in at least two situations: a) among the deep profile values (SW-C_{all} and SWC_{env}) and b) among the surface values (SWC_{hyd}) during the rainy periods.

The results of the comparison (Fig. 5) were considered satisfactory in terms of coefficient of determination ($R^2 > 0.6$) for all stations except for the fallow category and one isolated station (I6). There are no meaningful differences between the three alternatives of validation in terms of determination coefficient (Fig. 5a). Therefore, we can conclude that the simulation is useful for correctly characterizing the mean profile SWC as well as the surface level SWC. But the higher RMSE at Fig. 5b indicated a worse fitting with the surface values in most of the stations, and the fluctuating sign of the bias at this level (Fig. 5c) indicates that the simulation may barely predict the higher variability at the surface, whereas the bias for the profile-averaged content is always a dry bias.

The estimation improved if the simulated SWC was averaged for each land use/land cover and for the whole area (Table 2). The area-averaged simulation agrees bet-
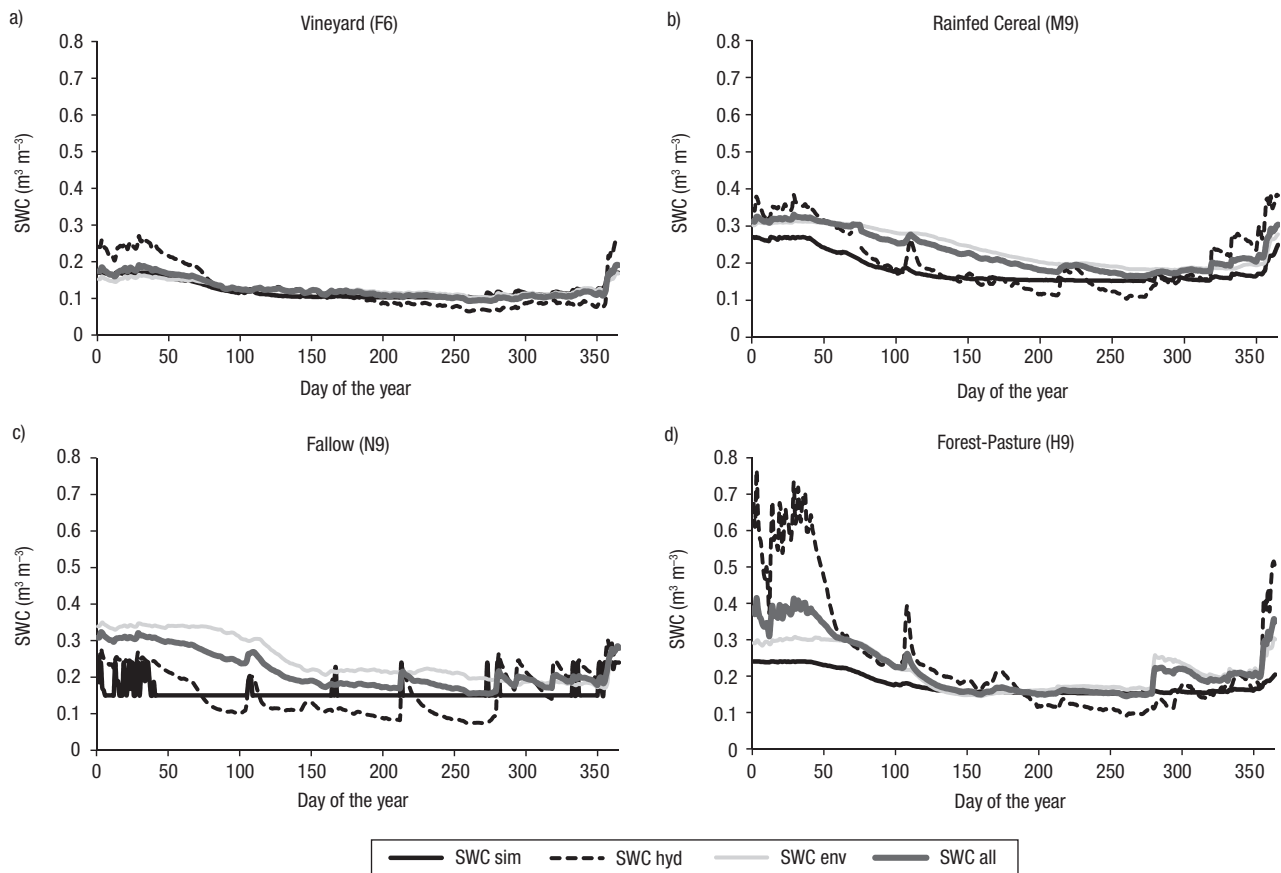
Figure 4. Simulated water content (SWCsim), and observed soil water content in the three alternatives, SWC_{hyd}; SWC_{all} and SWC_{env}, for vineyards (a), fallow (b), forest-pasture (c), and rainfed cereals (d).

ter with both the mean observations at surface level ($R^2 = 0.94$, RMSE = 0.041 $m^3 m^{-3}$, and bias = –0.002 $m^3 m^{-3}$) and the profile-average ($R^2 = 0.86$, RMSE = 0.037 $m^3 m^{-3}$, and bias = –0.034 $m^3 m^{-3}$ for SWC_{env}; and $R^2 = 0.92$, RMSE = 0.031 $m^3 m^{-3}$, and bias = –0.027 $m^3 m^{-3}$ for SWC_{all}). As stated before, the underestimation is still clearer for the profile-averaged than for the surface values. Regarding the categories best characterized, the simulation is slightly better for vineyards and for rainfed cereals. The comparison cannot be done over forest-pasture because only one EnviroSMART profile is located in this land use (H9), which represents an isolated value. However, the error for this category at surface level is the largest (RMSE = 0.117 $m^3 m^{-3}$).

Discussion

Many researchers have studied the relationship between root growth and soil water (Quanqi *et al.*, 2010) because uncertainties come mainly from the high variability of soil properties and root depth (Ju *et al.*, 2010; Sánchez *et al.*, 2010). These parameters of soil properties and root activity have shown to be the most important parameters affecting the SWC on a small scale. The dependence of root activity in this model is verified here through the failure of the simulation over fallow or bare soil plots. The present work used SWC as control variable of the water balance in a profile-based observation. Since the *in situ* observations were made at different depths, the single value of simulated SWC can be checked against the vertical profile; in particular we used the upper topsoil values and the profile-averaged. The simulation represents fairly well the SWC dynamics compared with both the surface curve and the soil profile, but the bias is reduced when comparing the simulated SWC with the profile-averaged SWC (SWC_{all}). The underestimation observed in Sánchez *et al.* (2010) was also detected in this case because the profile-averaged SWC is clearly underestimated in eight of the twelve stations. As suggested there, there is a need to redefine the limits of the plant
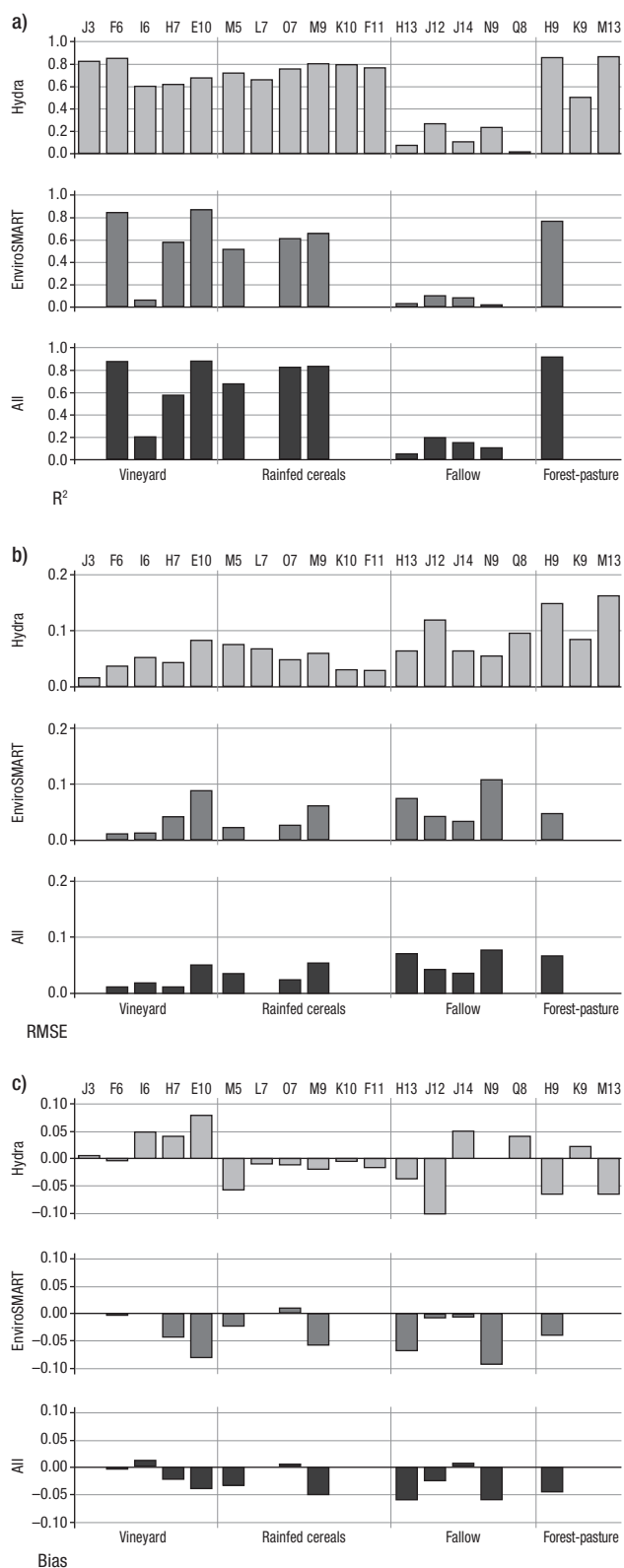
Figure 5. Determination coefficient R^2 (a), root mean square error, RMSE (b), and bias (c) for each station and category in the three alternatives of validation.

available water used in the calculation, which in turn depends on the field capacity and the wilting point. However, the RMSE obtained here, ranging between 0.011 and 0.149 $m^3 m^{-3}$, is in line with similar works (Diekküger *et al.*, 1995; Vanclooster & Boesten, 2000; Jalota & Arora, 2002; Zhang & Wegehenkel, 2006), and with remotely sensed estimations of soil moisture, such as SMOS (Soil Moisture and Ocean Salinity from the European Space Agency) and SMAP (Soil Moisture Active-Passive from NASA), targeted in an RMSE of 0.04 $m^3 m^{-3}$.

It is necessary to note the higher RMSE values in the case of the three forest-pasture stations at surface layer. The RMSE was 0.149, 0.085 and 0.164 for H9, K9 and M13, respectively. These errors can be explained for the specific location of these stations in the bottoms of the valleys, near the stream water, where the water table is shallow in winter, flooding occasionally occurs, and there is a higher content of clay in soils. In these cases, the actual SWC could reach higher values than the SWC_{FC} in some periods, and these conditions cannot be explained by the standard calculation of FAO56. Another explanation is that the FAO56 method is generally limited to applications with crops, although it can be applied to natural vegetation with greater uncertainty in the crop coefficient (Allen & Bastiaanssen, 2005) or woody crops such as vineyards (Campos *et al.*, 2010). However, experience suggests that the most influential parameter in the water balance is the water retention capacity, expressed in terms of SWC_{FC}, and the root depth. In the application of a distributed, physically based model, Rößler & Löffler (2010) found that soil moisture was especially sensitive to changes of soil parameters, and here, the most critical parameter seemed to be the SWC_{FC}, the upper limit of plant water availability.

In previous experiments of soil moisture estimations in REMEDHUS (Ceballos *et al.*, 2005; Wagner *et al.*, 2007b; Sánchez *et al.*, 2010), the soil moisture was observed every two weeks, whereas a daily averaged interval was used here. This new interval matches the time interval of the calculation and improves the reliability of the validation process because the potential variability of both curves is expected to be similar. In the present study, the simulated soil moisture shows a good agreement (total-averaged SWC with $R^2 = 0.94$, 0.86 and 0.92 for SWC_{hyd}, SWC_{env} and SWC_{all}, respectively), whereas the values are mostly underestimated (bias negative), especially in the

Table 2. Determination coefficient, R^2, root mean square error (RMSE, $m^3 m^{-3}$), and bias ($m^3 m^{-3}$) for each category (averaged and the total) averaged in the three alternatives of validation. There is no average for forest-pasture because there is only one station with both sensors

	Hydraprobe			EnviroSMART			All		
	R^2	RMSE	Bias	R^2	RMSE	Bias	R^2	RMSE	Bias
Average	0.94	0.041	− 0.002	0.86	0.037	− 0.034	0.92	0.031	− 0.027
Forest-Pasture	0.85	0.117	− 0.038						
Rainfed cereals	0.85	0.039	− 0.013	0.79	0.029	− 0.022	0.86	0.030	− 0.025
Vineyard	0.87	0.035	0.033	0.83	0.033	− 0.031	0.86	0.016	− 0.013

forest-pasture areas (RMSE = 0.117 $m^3 m^{-3}$ and bias = −0.038 $m^3 m^{-3}$). This underestimation is in general clearer when comparing the simulated SWC with the whole profile average due to its higher water content. For the same reason, the underestimation was more pronounced during the wet season, *i.e.,* winter; reaching bias above −0.40 $m^3 m^{-3}$ for forested stations such as H9 in this period (Fig. 4). High values of water content may have been hindered by the limit of the SWC_{FC} established in the simulation.

It can be concluded that the simulation better described the dynamics of surface SWC, in terms of R^2, than at the deeper layers, but the errors are higher (Table 2) and more variable (Fig. 5). The best simulation took place for vineyards and rainfed cereals. One limitation is that the relationship between remote VI and crop coefficients were based on the basal crop coefficient K_{cb}, which is defined when the soil surface is dry but transpiration is occurring at potential rate (Allen *et al.*, 1998). These conditions are particularly present in herbaceous crops (*e.g.,* cereals), due to this high fraction of coverage (minimum soil evaporation), and during the growing cycle (*i.e.,* March to June), free of water stress in the root zone. This fact could explain the good results of the approach in this area, due to the predominance of this coverage, and the poor agreement over the fallow areas. These conditions are not present over vineyards, on the contrary, there is a wide area of bare soil among plants, with scarce water supply during their development stage. Even though, the simulation seems to be quite accurate for these stations in average ($R^2 = 0.92$, RMSE = 0.031 $m^3 m^{-3}$, bias = −0.027 $m^3 m^{-3}$). It could be possible that the low water contents in these sandy soils would mask the errors of the estimation. Working under non-stressed and reduced evaporation conditions, Campos *et al.* (2010) obtained a good agreement of simulated AET over vineyards using a linear relationship NDVI-K_{cb}. These findings support the possibility of an accurate application of the remotely sensed K_c-ET_0 methodology, and it opens the suite of crops for which its application is suitable.

The hypothesis of the suitability of HIDROMORE+ and the NDVI-K_{cb} approach for the distributed calculation of hydrological variables, particularly SWC, has been tested using the database of the REMEDHUS network (Duero basin, Spain). The results have been very satisfactory, especially in agricultural areas (vineyard and rainfed cereals), in terms of averaged SWC for the whole area. In the fallow areas, where the root activity is absent or limited, the calculation failed. Indeed, the critical parameters of the SWC calculation have proven to be the root depth and the upper limit of the SWC considered by the model. This limit, established as the water content at field capacity, prevents higher values of SWC in the simulation. Hence, the forest-pasture cover showed an underestimation of the surface SWC, and a general underestimation around −0.030 $m^3 m^{-3}$ is detected for all the stations in the root zone, more clear during the wet period.

The procedure described in this paper for estimating soil water content and other components of the water balance opens the possibility of combining the measured point-data with imagery products from other optical, thermal or radar bands and sensors to increase the accuracy of the spatially distributed water balance. Obtaining an accurate distributed water balance is the main hydrological challenge for many practical and theoretical purposes related with water management and irrigation schemes along a wide range of scales.

Acknowledgements

References

Allen RG, 2000. Using the FAO-56 dual crop coefficient method over an irrigated region as part of an evapotranspiration intercomparison study. J Hydrol 229(1-2): 27-41.

Allen RG, Bastiaanssen WGM, 2005. Editorial: Special issue on remote sensing of crop evapotranspiration for large regions. Irrig Drain Syst 19(3-4): 207-210.

Allen RG, Pereira LS, Raes D, Smith M, 1998. Crop evapotranspiration. FAO, Rome. 300 pp.

Bausch WC, Neale CU, 1987. Crop coefficients derived from reflected canopy radiation: a concept. T Am Soc Agric 30(3): 703-709.

Bonet L, Ferrer P, Castel JR, Intrigliolo DS, 2010. Soil capacitance sensors and stem dendrometers. Useful tools for irrigation scheduling of commercial orchards? Span J Agric Res 8(S2): S52-S65.

Calera A, González-Piqueras J, Meliá J, 2004. Monitoring barley and corn growth from remote sensing data at field scale. Int J Remote Sens 25(1): 97-109.

Campos I, Neale CMU, Calera A, Balbontín C, González-Piqueras J, 2010. Assessing satellite-based basal crop coefficients for irrigated grapes (*Vitis vinifera* L.). Agr Water Manage 98(1): 45-54.

Ceballos A, Scipal K, Wagner W, Martínez-Fernández J, 2005. Validation of ERS scatterometer-derived soil moisture data in the central part of the Duero Basin, Spain. Hydrol Process 19(8): 1549-1566.

Chavez PS Jr, 1989. Radiometric calibration of Landsat Thematic Mapper multispectral images. Photogramm Eng Rem S 55(9): 1285-1294.

Diekküger B, Söndgerath D, Kersebaum KC, Mcvoy CW, 1995. Validity of agroecosystem models—a comparison of results of different models applied to the same data set. Ecol Modelling 81(1-3): 3-29.

Earls J, Dixon B, Candade N, 2006. A comparative study of Landsat 5 TM land use classification methods including unsupervised classification, artificial neural network and support vector machine for use in a simple hydrologic budget model. ASPRS 2006 Ann Conf, Reno, NV, USA, May, 1-5.

Eitzinger J, Marinkovic D, Hösch J, 2002. Sensitivity of different evapotranspiration calculation methods in different crop-weather models. Proc. First Biennial Meeting of the International Environmental Modelling and Software Society, Manno, Switzerland, June, 24-27. pp: 395-400.

Er-Raki S, Chehbouni A, Guemouria N, Duchemin B, Ezzahar J, Hadria R, 2007. Combining FAO-56 model and ground-based remote sensing to estimate water consumptions of wheat crops in a semi-arid region. Agr Water Manage 87(1): 41-54.

Er-Raki S, Chehbouni A, Duchemin B, 2010. Combining satellite remote sensing data with the FAO-56 dual approach for water use mapping in irrigated wheat fields of a semi-arid region. Remote Sens 2(1): 375-387.

Gonzalez-Dugo MP, Mateos L, 2008. Spectral vegetation indices for benchmarking water productivity of irrigated cotton and sugarbeet crops. Agr Water Manage 95(1): 48-58.

Grayson RB, Moore I, McMohan, TA, 1992a. Physically based hydrologic modeling 1. A terrain-based model for investigative purposes. Water Resour Res 28(10): 2639-2658.

Grayson RB, Moore I, McMohan TA, 1992b. Physically based hydrologic modeling 2. Is the concept realistic? Water Resour Res 28(10): 2659-2666.

Hunsaker DJ, Pinter PJ Jr, Kimball BA, 2005. Wheat basal crop coefficients determined by normalized difference vegetation index. Irrig Sci 24(1): 1-14.

Jalota SK, Arora VK, 2002. Model-based assessment of water balance components under different cropping systems in north-west India. Agr Water Manage 57(1): 75-87.

Ju W, Gao P, Wanga J, Zhou Y, Zhang X, 2010. Combining an ecological model with remote sensing and GIS techniques to monitor soil water content of croplands with a monsoon climate. Agr Water Manage 97(8): 1221-1231.

Liu Y, Luo Y, 2010. A consolidated evaluation of the FAO-56 dual crop coefficient approach using the lysimeter data in the North China Plain. Agr Water Manage 97(1): 31-40.

López-Urrea R, Montoro A, González-Piqueras J, López Fuster P, Fereres E, 2009. Water use of spring wheat to raise water productivity. Agr Water Manage 96(9): 1305-1310.

Martín De Santa Olalla F, Calera A, Domínguez A, 2003. Monitoring irrigation water use by combining irrigation advisory service and remotely sensed data with a geographic information system. Agr Water Manage 61(2): 111-124.

Martínez-Fernández J, Ceballos A, 2003. Temporal stability of soil moisture in a large-field experiment in Spain. Soil Sci Soc Am J 67(6): 1647-1656.

Martínez-Fernández J, Ceballos A, 2005. Mean soil moisture estimation using temporal stability analysis. J Hydrol 312(1-4): 28-38.

Neale CM, Bausch WC, Heerman DF, 1989. Development of reflectance-based crop cofficients for corn. T ASAE 32(6): 1891-1899.

Quanqi L, Baodi D, Yunzhou Q, Mengyu L, Jiwang Z, 2010. Root growth, available soil water, and water-use efficiency of winter wheat under different irrigation regimes applied at different growth stages in North China. Agr Water Manage 97(10): 1676-1682.

Rößler O, Löffler J, 2010. Potentials and limitations of modelling spatio-temporal patterns of soil moisture in a high mountain catchment using WaSiM-ETH. Hydrol Process 24(15): 2182-2196.

Rouse JW, Haas RH, Shell JA, Deering DW, Harlan JC, 1974. Monitoring the vernal advancement of retrogradation of natural vegetation. Final Report, Type III. Greenbelt, MD, NASA/GSFC. 371 pp.

Sánchez N, Martínez-Fernández J, Calera A, Torres EA, Pérez-Gutiérrez C, 2010. Combining remote sensing and in situ soil moisture data for the application and validation of a distributed water balance model (HIDROMORE). Agr Water Manage 98(1): 69-78.

Shepard D, 1968. A two-dimensional interpolation function for irregularly-spaced data. Proc. 23rd ACM Nat Conf, NY. pp: 517-524.

Singh UK, Rena L, Kang SZ, 2010. Simulation of soil water in space and time using an agro-hydrological model and remote sensing techniques. Agr Water Manage 97(8): 1210-1220.

Torres EA, Calera A, 2010. Bare soil evaporation under high evaporation demand: a proposed modification to the FAO-56 model. Hydrolog Sci J 55(3): 303-315.

Toutin T, 2004. Geometric processing of remote sensing images: models, algorithms and methods (review). Int J Remote Sens 25(10): 1893-1924

Van Genuchten MT, 1980. A closed form equation for predicting the hydraulic conductivity of unsaturated soils. Soil Sci Soc Am J 44(5): 892 898.

Vanclooster M, Boesten J, 2000. Application of pesticide simulation models to the Vredepeel dataset I. Water, solute and heat transport. Agr Water Manage 44(1-3): 105-117.

Vincent S, Pierre F, 2003. Identifying main crop classes in an irrigated area using high resolution image time series. Proc. IEEE Int Geosci Remote Sens Symp, IGARSS 2003, Toulouse, France, July 21-25. pp: 252-254.

Wagner W, Blöschl G, Pampaloni P, Calvet JC, Bizzarri B, Wigneron JP, Kerr Y, 2007a. Operational readiness of microwave remote sensing of soil moisture for hydrologic applications. Nord Hydrol 38(1): 1-20.

Wagner W, Naeimi V, Scipal K, De Jeu R, Martínez-Fernández J, 2007b. Soil moisture from operational meteorological satellites. Hydrogeol J 15(1): 121-131.

Western A, Grayson RB, 2000. Soil moisture and runoff processes at Tarrawarra. In: Spatial patterns in catchment hydrology: observations and modelling. Cambridge Univ Press, Cambrigde, UK, pp: 209-246.

Wright JL, 1982. New evapotranspiration crop coefficients. J Irrig Drain Div 108(1): 57-74.

Zhang Y, Wegehenkel M, 2006. Integration of MODIS data into a simple model for the spatial distributed simulation of soil water content and evapotranspiration. Remote Sens Environ 104(4): 393-408.